

---

# STABILIZATION OF THE INJECTION LOCKING OF A SEMICONDUCTOR LASER DIODE

Semester Thesis

---

Physics Master's Degree at ETH Zürich  
Ion Trap Quantum Computing Group  
Paul Scherrer Institute

## Supervision

Julian Schmidt  
Luka Milanovic  
Prof. Jonathan Home

## ABSTRACT

---

Injection-locking of a semiconductor laser diode is a practical and cost-effective way of amplifying a primary laser while keeping its spectrum intact. When the power of the primary laser is small, active stabilization of the current sent to the laser diode can increase the long-term stability of the injection-locking.

Here, we report the first application of a polarization spectroscopy stabilization technique on the injection-locking of a semiconductor laser diode. This stabilization technique is studied in detail and results in the stability of the injection-locking of  $20 \mu\text{W}$  of primary laser's power for more than 4 hours against a few minutes without any stabilization technique. This technique is based on the Hänsch-Couillaud scheme for stabilizing cavities and only requires a few additional optical elements to stabilize an already existing injection-locking setup. We also study in detail the influence of the seed power, output power, and temperature on the passive stability of the injection locking. The results presented in this thesis can serve as a tool to find the optimum operating conditions of an injection-locking setup.

# CONTENTS

---

<b>Introduction</b>	<b>4</b>
<b>I Injection locking of a semiconductor laser diode</b>	<b>5</b>
I.1 Theory of injection locking . . . . .	5
I.2 Experimental setup . . . . .	8
I.2.1 Initiating the laser diode . . . . .	8
I.2.2 Spectral purity of the injection . . . . .	11
I.2.3 Current and Temperature settings for the injection-locking . . . . .	11
<b>II Active stabilization of the injection</b>	<b>13</b>
II.1 Basic operation of feedback loops . . . . .	13
II.2 Examples of stabilization schemes of the injection-locking . . . . .	13
II.2.1 Fabry-Perot Interferometer . . . . .	14
II.2.2 Narrow-band filter . . . . .	14
II.3 Hänsch-Couillaud scheme . . . . .	16
II.3.1 Basic idea . . . . .	16
II.3.2 Experimental setup . . . . .	19
II.3.3 Understanding the obtained error signal: . . . . .	22
II.4 Optimizing the feedback loop . . . . .	23
<b>III Increasing the passive stability of the injection-locking</b>	<b>25</b>
III.1 Injection range versus seed power and output power of the diode . . . . .	25
III.1.1 Injection range versus Seed power . . . . .	25
III.1.2 Injection range versus Output power . . . . .	25
III.2 Influence of the temperature . . . . .	27
III.2.1 Influence of the temperature on the beam profile and direction of propagation . . . . .	27
III.2.2 Influence of the temperature on the gain spectrum . . . . .	28
<b>IV Spectrum of the amplified light</b>	<b>31</b>
IV.1 Setting up a beat note setup . . . . .	31
IV.2 Beat note spectrums . . . . .	31
IV.2.1 Beat note spectrums obtained with different current controllers . . . . .	31
IV.2.2 Other beat note spectrums . . . . .	33
<b>V Conclusion</b>	<b>34</b>
<b>VI Acknowledgements</b>	<b>35</b>

# INTRODUCTION

---

In a trapped ion experiment, individual ions are confined and manipulated using electromagnetic fields. Laser beams are integral to this process, performing a variety of functions including cooling the ions, initializing quantum states, performing quantum gate operations, and reading out the state of the qubits. Each of these tasks, especially qubit manipulations, requires lasers with extremely stable frequencies, narrow linewidths, and precise tuning capabilities

To achieve the level of precision required, one effective method is the injection-locking of laser diodes. Injection-locking is a technique where a primary (seed) laser with excellent frequency stability and narrow linewidth is used to control the output of a secondary laser diode. The secondary laser, when injected with a small portion of the primary laser's output, locks its frequency to that of the primary laser, thereby inheriting its spectral purity and stability.

This technique offers several advantages. First, it allows for the amplification of the seed laser's light without compromising its coherence properties, thereby providing higher output power while maintaining the desired spectral characteristics. Second, the approach is cost-effective and scalable, as it leverages commercially available semiconductor laser diodes, which are compact, efficient, and relatively inexpensive compared to other high-performance laser systems

The transmitted light of a high-finesse cavity is an excellent choice for a seed laser in injection-locking due to its exceptional frequency stability and narrow linewidth. High-finesse cavities are designed to have very low loss, resulting in extremely narrow resonance peaks. This narrow linewidth ensures that the light exiting the cavity maintains a highly stable frequency with minimal noise. The power of the light transmitted through a high-finesse cavity is generally extremely small (less than  $100 \mu\text{W}$ ), but the injection-locking of a semiconductor laser diode has the advantage of requiring very little power from the seed laser. This enables the possibility of making use of this transmitted light as an extremely stable laser beam after several amplification stages.

The seed laser that will be ultimately used has a power of tens of  $\mu\text{W}$ . In this small power regime, the current sent to the secondary laser diode for the injection locking needs to be tuned with a precision of less than  $50 \mu\text{A}$ . Hence, the goal of this project is two-fold. We characterize the stability of the injection-locking as a guide to find the optimum operating conditions of the laser diode and maximize the passive stability of the injection-locking. Furthermore, we describe a cost-effective and practical technique to actively stabilize the injection-locking via a feedback loop.

In this thesis, we will first introduce the concept of injection-locking by going through the theory and the basic experimental setup used. We will then describe a technique, based on the Hänsch-Couillaud stabilization scheme for cavities, to actively stabilize the current sent to the laser diode for injection-locking. The following section will be dedicated to characterizing the passive stability of the injection-locking. Finally, we will compare the spectrum of the primary laser with the spectrum of the light amplified with the injection-locking.



# I INJECTION LOCKING OF A SEMICONDUCTOR LASER DIODE

## I.1 THEORY OF INJECTION LOCKING

A semiconductor laser diode (LD) is made of a p-n junction, acting as a gain medium, surrounded by two mirrors forming a Fabry-Perot cavity, selecting the lasing frequencies of the LD. The free-running lasing mode of the LD is determined by a competition between all the frequencies  $n\nu_{FSR}$  allowed by the Fabry-Perot cavity whose gain gets above the gain threshold. The LD is mainly controlled by two parameters: its temperature, and the current sent through the p-n junction. The temperature shifts the gain spectrum and so the frequency of the LD. The current changes the density of charge carriers inside the p-n junction, increasing the gain and so the output power of the LD. A modification of the charge carrier density also changes the refractive index of the material, and so does the effective length of the Fabry-Perot cavity. Thus, The frequency of the LD is modified by both the temperature and the current.

While an LD typically starts lasing when spontaneously emitted photons get amplified by the gain medium, one can also drive the LD by injecting photons inside the cavity. If the frequency of these injected photons is resonant with the Fabry-Perot cavity and if the rate of their arrival surpasses the rate of spontaneous emission, then the injected light wins the mode competition inside the LD. The LD is thus 'injection-locked', and the spectrum of the emitted light is, in theory, the same as that of the seed light. We call the 'injected LD light' the light emitted by the LD when it is injection-locked by a primary laser (PL).

For the PL to drive efficiently the LD, its frequency needs to be resonant with the Fabry-Perot cavity of the LD. Therefore, injection-locking can only happen at certain values of the current and temperature of the LD.

We will, in the rest of this section, briefly derive the equations describing the field inside the cavity when light is injected. These derivations follow the example of [1].

For simplicity, we assume that the LD is running single-mode at the frequency  $\omega_q$ , such that the intra-cavity field is written  $E(t) = A(t)e^{-i\omega_q t}$ . The differential equation describing the evolution of the amplitude of the field  $A(t)$  without the presence of seed light is:

$$\frac{dA}{dt} = -\frac{A}{2\tau_{cav}} \left( 1 - \frac{r}{1 + \frac{2|A|^2}{I_{sat}}} \right) \quad (1)$$

$\tau_{cav}$  is the rate of photons leaking out of the cavity.  $I_{sat}$  is the saturation intensity of the gain medium.  $r$  is the excitation ratio between the unsaturated gain per round trip and the losses (typically,  $r$  depends on the current sent to the diode, and  $r > 1$  is a necessary lasing condition).

The steady-state solution of this equation gives the free-running amplitude of the light field:  $|A_0|^2 = \frac{I_{sat}}{2}(r - 1)$ .

Now suppose that seed light with a frequency  $\omega_1$  is injected inside the diode such that we now write the intra-cavity field  $E(t) = A(t)e^{-i\omega_1 t}$ . We write  $A_1$  the PL field incident on the mirror (which we take real without loss of generality), and  $\frac{1}{\tau_{inj}} = \frac{c}{L_{cav}}T_1$  the arrival rate of seed photons inside the cavity.  $L_{cav}$  is the length of the cavity,  $c$  is the speed of light (we assume that the refractive index is equal to 1 for simplicity), and  $T_1$  is the transmission coefficient of the first mirror of the cavity. In the presence of the seed light, equation (1) is transformed as:

$$\frac{dA}{dt} = -\frac{A}{2\tau_{cav}} \left( 1 - \frac{r}{1 + \frac{2|A|^2}{I_{sat}}} \right) + i(\omega_1 - \omega_q)A + \frac{1}{2\tau_{inj}}A_1 \quad (2)$$

We can then write  $A = |A|e^{i\phi}$  and get equations for the amplitude and phase of the field:

$$\frac{d|A|}{dt} = -\frac{|A|}{2\tau_{cav}} \left( 1 - \frac{r}{1 + \frac{2|A|^2}{I_{sat}}} \right) + \frac{1}{2\tau_{inj}}A_1 \cos(\phi) \quad (3)$$

$$\frac{d\phi}{dt} = \omega_1 - \omega_q - \frac{1}{2\tau_{inj}} \left| \frac{A_1}{A} \right| \sin(\phi) \quad (4)$$

Assuming a weak seed light, we can neglect the second term in (3), leading to the same steady state solution for the amplitude of the field with or without injection. Therefore, we can replace  $|A|$  with  $|A_0|$  in (4) and get Adler's equation for the phase of the injected light:

$$\frac{d\phi}{dt} = \omega_1 - \omega_q - \Delta\omega \sin(\phi) \quad (5)$$

If  $|\omega_1 - \omega_q| \leq \Delta\omega$ , this equation has a steady state solution and the LD can lase at the same frequency as the PL.  $\Delta\omega = \frac{1}{2\tau_{cav}} \left| \frac{A_1}{A_0} \right|$  is therefore the injection range. One can already see its dependencies on the output power of the LD (proportional to  $|A_0|^2$ ), and on the seed power (proportional to  $|A_1|^2$ ). The effective injection range will be measured later in this thesis, and these two dependencies will be retrieved.

The steady-state solution for the phase of the LD field within the injection range is given by:

$$\sin(\phi) = \frac{\omega_1 - \omega_q}{\Delta\omega} \quad (6)$$

However, this simplified theoretical picture does not take into account the dependency of the refractive index of the gain medium on the charge carrier density. A more complete model is derived in [2]. We write  $\alpha$  the linewidth enhancement factor: a dimensionless parameter proportional to  $\frac{\partial n}{\partial N}$ , where  $n$  is the phase refractive index and  $N$  is the charge carrier density. From [2], the injection range is now  $\Delta\omega\sqrt{1 + \alpha^2}$ , and the steady state phase shift between the injected LD light and the seed light is

$$\phi = -\arctan(\alpha) + \arcsin\left(\frac{\omega_1 - \omega_q}{\Delta\omega\sqrt{1 + \alpha^2}}\right) \quad (7)$$

The injection range is therefore enhanced, and more importantly, the phase shift between seed and injected LD light is not 0 at the perfect resonance between seed light and Fabry-Perot cavity mode. This will be important in section II.3.2.

Out of this injection range, there is still a solution to Adler's equation. The phase is no longer constant, and there is a frequency shift between the seed light and the injected LD light. The frequency of the injected LD can be obtained by rewriting (5):

$$\frac{d\phi}{\omega_1 - \omega_q - \Delta\omega \sin(\phi)} = dt \quad (8)$$

and integrating over one period  $T$ . One can find  $T = \frac{2\pi}{\sqrt{(\omega_1 - \omega_q)^2 - \Delta\omega^2}}$ , leading to the frequency:

$$\omega_{LD} = \sqrt{(\omega_1 - \omega_q)^2 - \Delta\omega^2} \quad (9)$$

The frequency of the injected LD light is plotted as a function of the PL frequency in Figure 1.

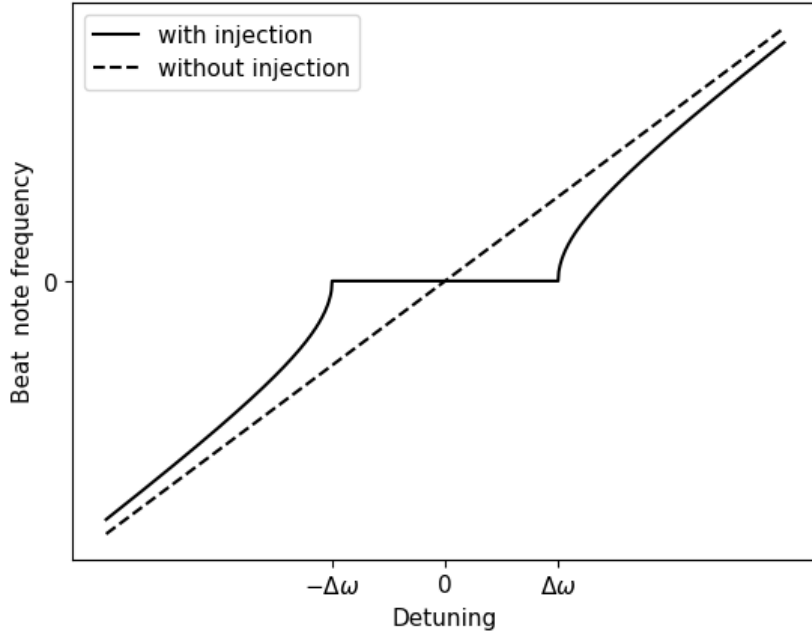


**Figure 1:** Beat note frequency between the primary laser and the laser diode as a function of the detuning between the primary laser and the free-running frequency of the laser diode. The beat note frequency is shown with and without injection.

Throughout all this derivation, we assumed that  $\omega_q$  was the free-running frequency of the LD, but the PL need not be resonant with the free-running mode for the injection to work. Being resonant with any mode of the Fabry-Perot cavity is enough. Then, whether there is or isn't an injection is a matter of mode competition between the mode described by the

previous equations and the free-running mode. Generally, the free-running mode has a higher unsaturated gain than the mode resonant with the PL light, but the injected photons from the seed light compensate for this lower gain and still allow the injection. From this physical picture of the injection-locking mechanism, we can already understand that there will be three regimes when injecting the seed light: the *clean injection* regime, when  $|\omega_1 - \omega_q| < \Delta\omega$ , the *bad injection* regime, when the injected photons help the mode with frequency  $\omega_{LD}$  (described by equation (9)) win the competition against the free-running mode, and finally the *free-running mode* when the cavity is not resonant with the seed light, such that the seed light photons don't change the free-running behavior of the LD.

## I.2 EXPERIMENTAL SETUP

### I.2.1 • INITIALIZING THE LASER DIODE

We used the Laser Diode HL7302MG from Thorlabs [3] which can lase between 720 nm and 740 nm. Figure 2a shows the output power of the LD versus the current sent to the diode. Figure 2b shows the free-running wavelength of the diode versus its temperature. This wavelength has been measured at a constant current with a wavemeter. Most of the measurements shown in this thesis were done at a temperature of around 25 °C, which is the temperature recommended by the manufacturer of the laser diode. At this temperature, the free-running diode has a wavelength slightly different from the seed light used for the injection-locking. The effect of this detuning will be discussed in a further section.

The injection locking requires coupling as much seed light as possible to the mode of the Fabry-Perot cavity of the LD. Hence, we need to use lenses to match the beam profiles of the PL and the LD.

A total of five lenses is used to collimate the LD's beam and match its waist with the waist of the seed light beam (see Figure 4). The bare output beam of the LD is highly divergent (respectively 9° and 18° on the parallel and orthogonal axis). We use a first lens with a focal length of 7.5 mm for collimation. We then used two cylindrical lenses of focal lengths -40 mm and +70 mm to re-shape the orthogonal waist for it to match the parallel waist. Finally, we used two spherical lenses of focal lengths 25.4 mm and 40 mm to match the LD's waist with the PL's waist of 1.4 mm.

Once these telescopes were set, we tested the beam matching by coupling the LD's beam to the same fiber coupler used to send the PL to the optical table. We obtained a coupling of 53%. It is much below the average fiber coupling achievable because even after the lens system, the LD's beam is not Gaussian. Figure 3 shows the beam profile of the output of the LD right after the lens system and 2 m after the lens system. We observe that even if the beam profile looks more or less Gaussian right after the lenses, it does not propagate as a Gaussian beam. It is a superposition of many longitudinal modes that propagate differently in free space. The

## I. INJECTION LOCKING OF A SEMICONDUCTOR LASER DIODE

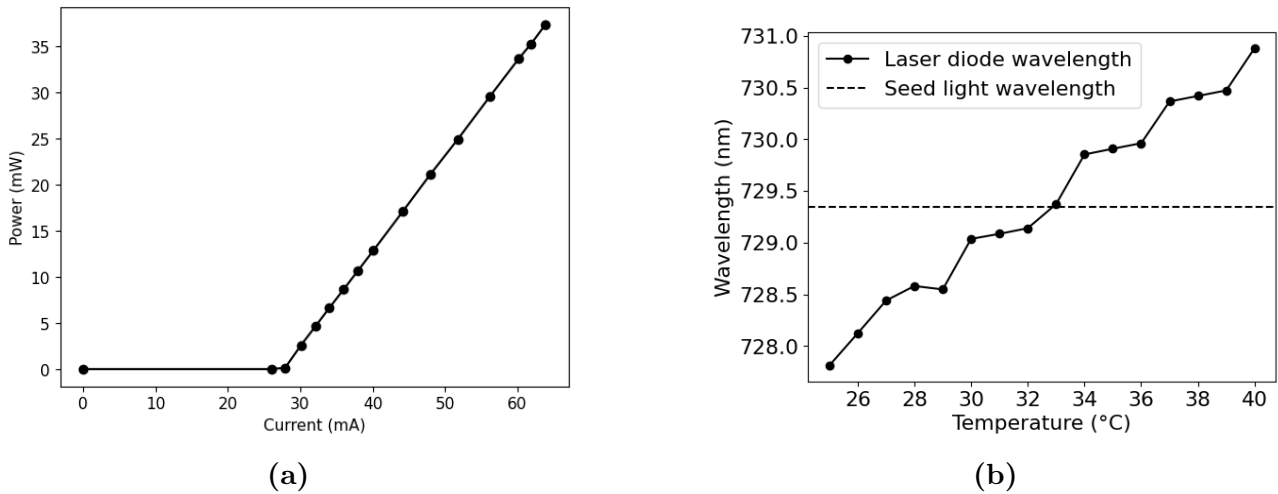


**Figure 2:** Figure 2a shows the output power of the laser diode as a function of the current sent to its controller. The data is taken at the temperature  $T=24.8$  °C. Figure 2b shows the wavelength of the free-running laser diode as a function of its temperature, with a constant current of 57 mA. The horizontal line shows the wavelength of the seed light we used to get most of the measurements of this thesis.

presence of these other longitudinal modes prevents a perfect mode matching between the seed light and the LD light.

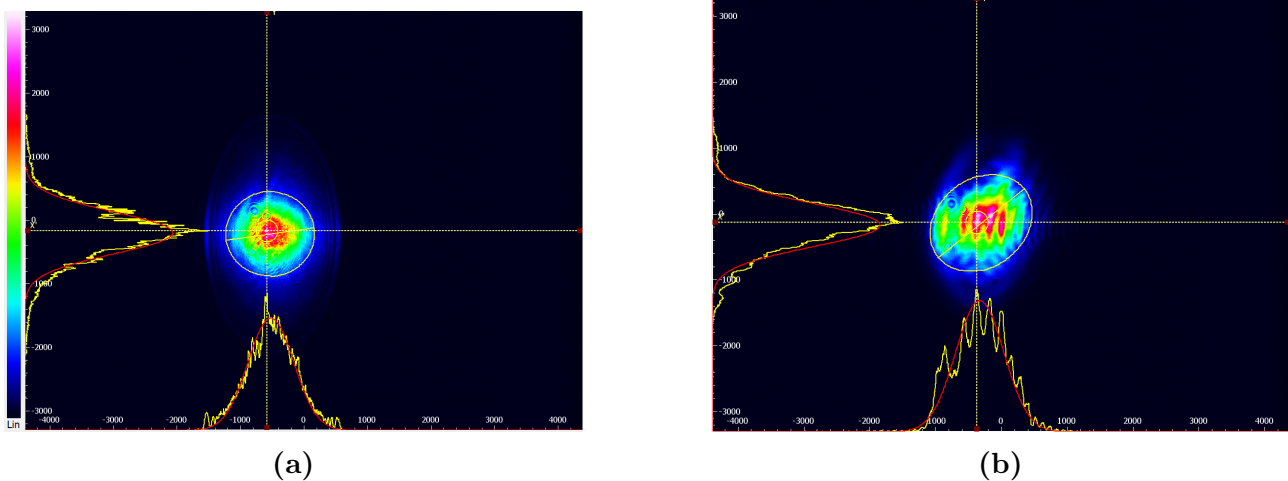


**Figure 3:** Beam profile of the laser diode output beam after the full lens system. Figure 3a shows the beam profile right after the lens system. Figure 3b shows the beam profile 2 m after the lens system

Figure 4 shows the initial setup used to inject seed light into the LD. We used a Fabry-Perot Interferometer (FPI) to verify the status of the injection. The free-running LD has a large linewidth, and its spectrum, measured by scanning the length of the FPI, is a weak broad

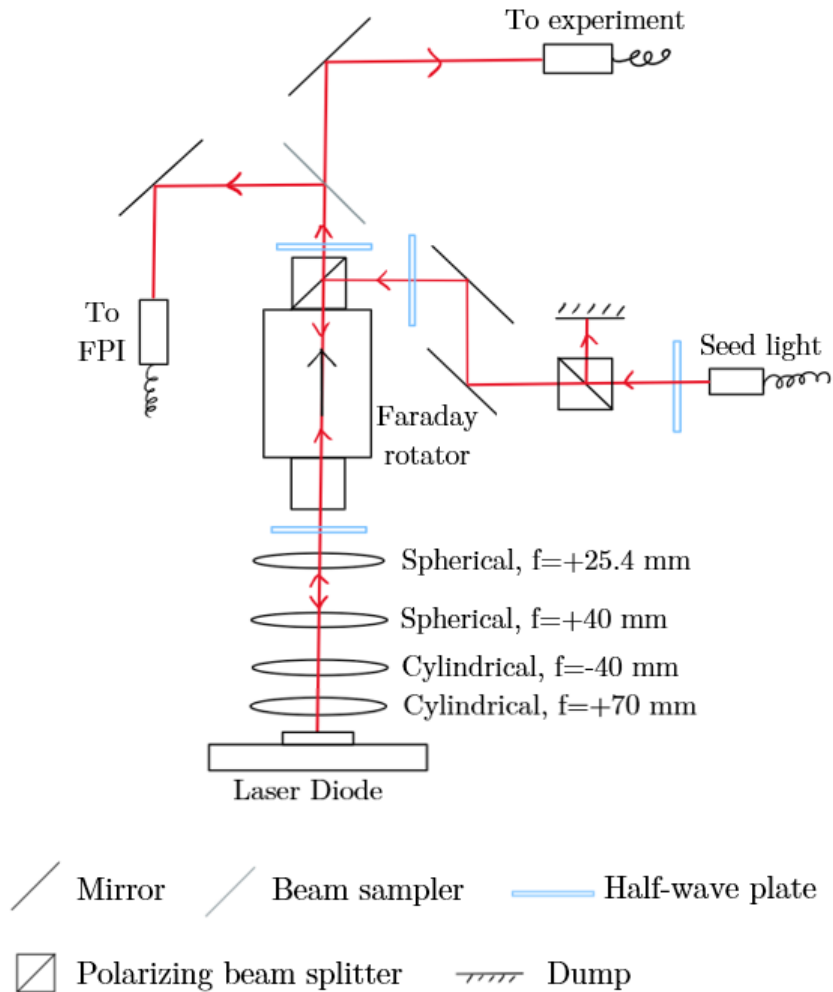


**Figure 4:** Diagram of the optical setup used to inject light from the primary laser to the laser diode. The  $f=+7.5$  mm lens used to collimate the beam out of the laser diode is not indicated, it is mounted directly on the laser diode mount. The distances are not to scale. A Fabry-Perot Interferometer (FPI) is used to monitor the injection status of the laser diode.

peak, whereas the PL spectrum is a high narrow peak. In the clean injection regime, the LD should have the same spectrum as the seed light. Thus, a radical change in the spectrum of the LD indicates that the current and temperature are correctly tuned and that the LD is injection-locked.

The Faraday isolator is used to prevent any back-reflected light from coming back to the LD's cavity and creating unwanted interferences.

We aligned the setup by coupling the light from the LD into the same collimator as the one used to send the seed light on the optical table. In principle, the Faraday isolator prevents light from the LD from taking this path, but if the LD power is 40 mW, there can still be some tens of  $\mu W$  going to the collimator, which is enough to be monitored with a power meter and hence to couple it to the collimator.

Throughout this project, we used an PL with an extremely good spectrum (sub-Hz linewidth) and "unlimited" seed power for a complete characterization of the injection locking.

### I.2.2 • SPECTRAL PURITY OF THE INJECTION

Since the free-running LD has a large linewidth, its power is distributed over a large range of frequencies. Hence, the intensity of the light transmitted through the FPI is significant only when the LD is injection-locked, and when its linewidth is significantly reduced. This transmitted intensity can be monitored and usually serves as a metric for the quality of the injection. Figure 5a shows the transmitted intensity around a clean injection current. The two vertical dashed lines limit the clean injection regime ( $|\omega_1 - \omega_q| < \Delta\omega$ ).

The asymmetric profile of the FPI transmission has been already discussed in [4, 5]. It can be explained by the dependency of the refractive index on the circulating current inside the LD. Starting from a resonance between the PL and the LD's cavity, increasing the current will increase the effective length, and so the resonant frequency, of the LD, hence driving the PL off-resonant and decreasing the circulating power inside the cavity. This decrease of the circulating power has the effect of decreasing the refractive index, and so the effective length of the LD's cavity. Hence, when increasing the current, the current and circulating power dependencies of the refractive index fight against each other, leading to an increased effective injection range. However, when decreasing the current starting from a resonance between the PL and the LD, these two effects will add up, and the PL will quickly jump off-resonance.

This effect also leads to a hysteresis phenomenon [4] and different effective injection ranges depending on whether the clean injection current is reached from downwards or upwards. We will in a further section demonstrate a more precise way of measuring the clean injection range than looking at the transmission of the FPI. Quantitative results will be given regarding this hysteresis phenomenon.

### I.2.3 • CURRENT AND TEMPERATURE SETTINGS FOR THE INJECTION-LOCKING

The LD's current needs to be correctly tuned to get the injection lock because the PL needs to be resonant with the LD's cavity. Changing the temperature of the diode shifts the length of the LD's cavity and so changes the current values at which resonance, and injection-locking, are obtained. Figure 5b shows a map of which current/temperature settings lead to the injection-locking of the LD.

Since the injection is obtained over a range of currents rather than at a single value, we did this measurement by decreasing significantly the seed power to reduce drastically this injection range down to a single value with a small error.

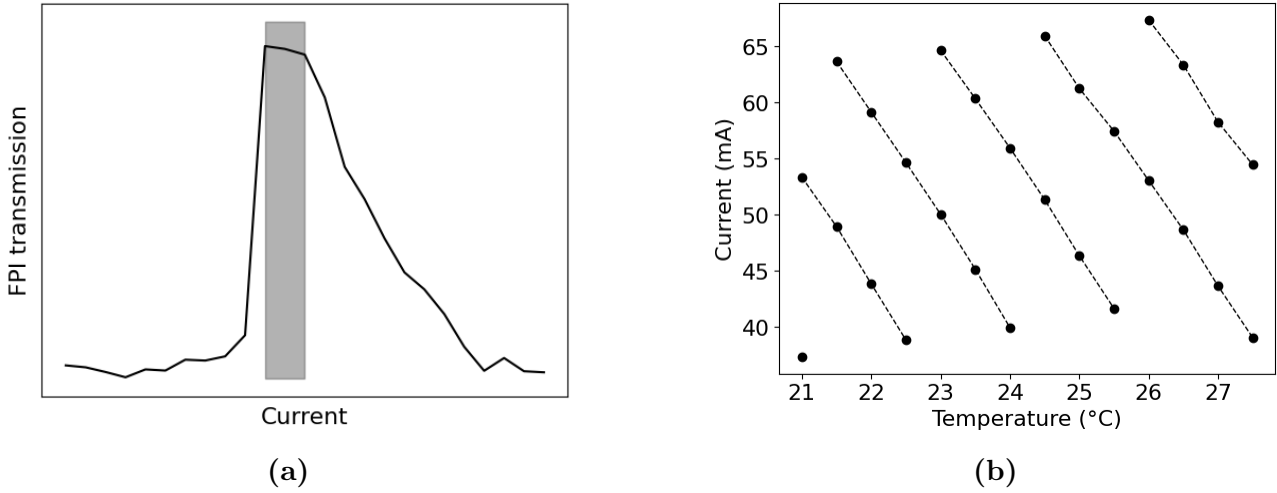


**Figure 5:** Figure 5a shows the maximum transmission through an FPI scanned over a full free-spectral range. The axes units are purely descriptive. The shaded region indicates the clean injection regime. In Figure 5b, each dot corresponds to a current and temperature settings at which the laser diode is injection-locked. Each dashed line corresponds to one resonance peak of the laser diode’s cavity being shifted by the temperature.

## II

# ACTIVE STABILIZATION OF THE INJECTION

---

Throughout the project, we used a temporary setup with as much seed light as necessary to analyze and understand better the principle of injection-locking. However, in real operation, the LD will be used to amplify light transmitted by a high-finesse Fabry-Perot cavity. This light has a narrow linewidth, but also a small power. Thus, the injection range when using this light will be quite small, and active stabilization of the current of the LD, using feedback loops, can help with long-term injection locking.

### II.1 BASIC OPERATION OF FEEDBACK LOOPS

---

We will not dive into too many details about feedback loops in this thesis, but a very complete description of them is given in [6].

A feedback loop is a technique that helps stabilize a physical quantity such as the frequency of a laser, the length of a cavity, or here, the frequency difference between the LD and PL. The naive idea to stabilize such quantity would be to measure it directly to know whether it is higher or lower than the desired value. The signal obtained can then be fed back to the system to get closer to the desired value. However, the frequency of a laser, for instance, has a value close to  $10^{15}$  Hz and needs to be stabilized with a precision below  $10^5$  Hz. A direct measurement of the frequency with a wavemeter would not be fast and precise enough to stabilize it. Therefore, people have come up with ideas like the Pound-Drever-Hall technique [7] to generate and measure an error signal meant to be proportional to the difference between the laser's frequency and the desired frequency. Over the range where this signal depends linearly on the quantity we want to stabilize, it is exactly equivalent to a direct measurement with, say, a wavemeter, but it can generally be measured faster and with more precision.

When it comes to injection locking, a lot of effort has been made to find a suitable error signal [5, 8, 9, 10, 11, 12]. The goal of this semester project was to investigate the technique presented in [9], based on the Hänsch-Couillaud (HC) stabilization scheme for cavities. We also compared this scheme with two other techniques that were easy to set up [5, 8].

### II.2 EXAMPLES OF STABILIZATION SCHEMES OF THE INJECTION-LOCKING

---

We will start by quickly presenting the stabilization techniques based on an FPI [5] and on a narrow-band filter [8], before explaining in more detail the Hänsch-Couillaud stabilization

scheme.

### II.2.1 • FABRY-PEROT INTERFEROMETER

The most common technique is probably to use an FPI to directly access the 'spectral purity' of the injected LD light. The idea is to send the LD light to an FPI to get a signal such as Figure 5a. The linear response of the error signal when the current is slightly higher than the clean injection regime is the part used for the feedback loop.

This technique is rather slow since limited by the time needed by the FPI to scan over a range large enough to be certain it contains the transmission peak of the injected light. Furthermore, the side-of-fringe locking stabilizes the current of the diode out of the clean injection regime, and some unwanted spectral modes can pollute the output of the LD.

This signal is however very convenient because it gives a direct measurement of the 'spectral purity' of the LD light, ie, a direct measurement of how clean the injection lock is.

### II.2.2 • NARROW-BAND FILTER

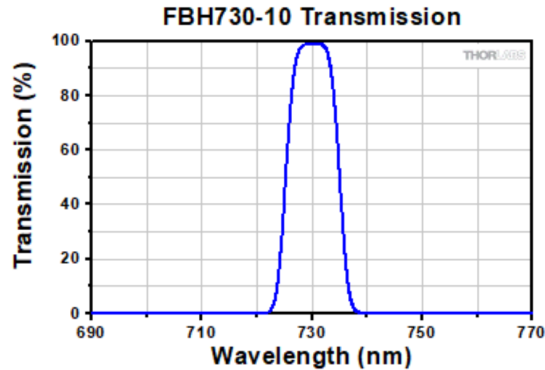
The next technique also uses side-of-fringe locking but allows for a much faster readout of the error signal. This technique, presented in [8] uses a narrow-band filter to filter out any light with a frequency different than the PPL frequency. If the free-running LD frequency is far from the PL frequency, then the narrow-band filter will transmit differently the LD light when it is injection-locked and the free-running LD light.

A narrow band filter is made of many layers of different lengths of dielectric material. It allows only a small range of frequencies to be transmitted thanks to destructive interferences of the other frequencies. The typical transmission spectrum for Thorlabs' filters is shown in Figure 6.

If the incident light hits the filter with an angle, then the effective length of the layers of dielectric in the filter will change, and the whole transmission spectrum will be shifted. This allows for more freedom in the selection of the transmitted/reflected frequencies by the filter.

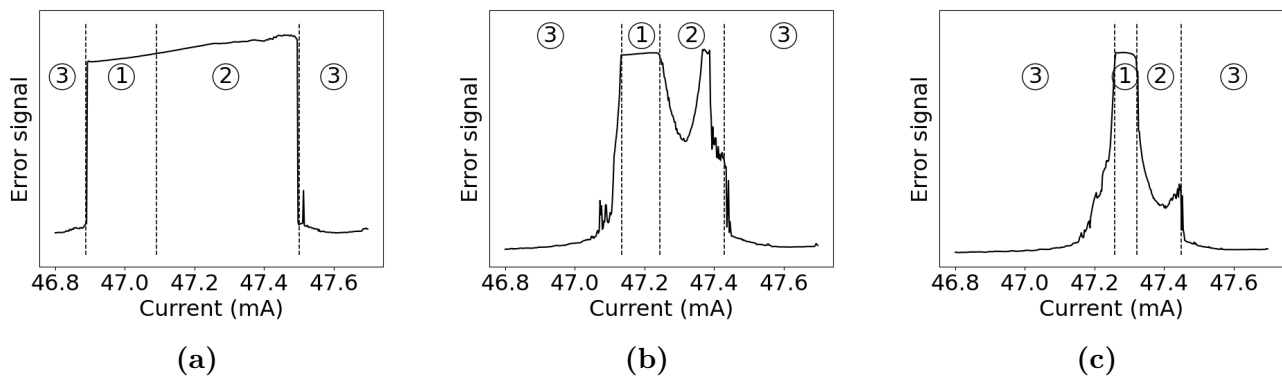
To try this technique, we first set the temperature of the LD such that its free-running wavelength is 1.5 nm below the PL's wavelength. Then, we shone the LD light on the filter with an incident angle such that the transmission of the free-running frequency is close to 100%, and the transmission of the PL frequency is close to 20%. We then measured the intensity of the reflected light to obtain a peak when the LD is injection-locked and a dip when it is free-running. The error signal obtained for different seed powers is shown in Figure 7.

Figure 7a shows the typical signal obtained at relatively high seed powers (400  $\mu W$  here). The injection status of the diode can be simultaneously monitored with the FPI, and the numbers in Figure 7 indicate the injection regime observed. 1 refers to the clean injection regime, 2 to the bad injection regime, and 3 to no injection (see part I.1 for the definition of these regimes). Since this signal is frequency dependent, it does not allow to differentiate



**Figure 6:** Data sheet from Thorlabs showing the transmission spectrum of the narrow-band filter FBH730-10 when used at normal incidence [3].

the clean and bad injection regimes when the seed power is high. Figure 7c and 7b however show that the transition between the clean and bad injection regimes is not smooth when the seed power is smaller. The decrease, followed by a 'revival' of the error signal when the seed power is smaller is not fully understood. The total power of the LD does not vary enough to explain such a change in the error signal. Hence, we understand it by a competition between the three modes (clean injection, bad injection, and free-running). The error signal getting lower indicates that the free-running mode wins the competition, while the 'revival' indicates that the 'bad injection' mode wins. This behavior strongly depends on the broad gain spectrum inside the p-n junction, which we don't know.



**Figure 7:** Error signals obtained by monitoring the reflection of the laser diode off the narrow-band filter for  $400 \mu W$  (7a),  $120 \mu W$  (7b), and  $60 \mu W$  (7c). The numbers indicate the three regimes of injection: 1 for the clean injection regime, 2 for the bad injection regime, and 3 for the free-running regime. Our definitions of these regimes are given in section I.1

If the free-running LD and PL have different enough frequencies, then reducing the seed power changes the shape of the error signal such that it is linear out of the clean injection range (as in Figure 7b). A side-of-fringe lock can then be performed, like with the FPI error signal. However, reducing the seed power leads to reducing the clean injection range, hence

## II. ACTIVE STABILIZATION OF THE INJECTION

to less stability. As with the FPI error signal, the LD is not locked inside the clean injection regime, but slightly out. Furthermore, these locks require arbitrarily setting a lock point which is highly dependent on the overall power, reducing their stability.

### II.3 HÄNSCH-COULLAUD SCHEME

The following locking scheme has been introduced in [9] to stabilize the injection locking of a cavity ring laser diode. To our knowledge, no experimental realization of this stabilization technique on a semiconductor laser diode has been published yet. However, Thomas Kinder from TEM Messtechnik has already successfully implemented this technique on a semiconductor laser diode, so we decided to try implementing it after a discussion with him.

As we will show in the next section, this new technique is similar to the Hänsch-Couillaud (HC) locking scheme [13] to lock a cavity to a laser or vice-versa. It has the advantages of being fast, easy to set up, and not locking on the side of the fringe of an error signal, hence achieving a perfect injection.

#### II.3.1 • BASIC IDEA

In this section, we will come back to the principle of the Hänsch-Couillaud locking scheme, as introduced in [13]. A good understanding of it is the cornerstone for analyzing the error signal obtained and optimizing it for locking the injection.

The HC scheme is used to lock the frequency of a laser to the length of a cavity in which a linear polarizer has been placed. The polarization parallel to the polarizer, which we write  $|H\rangle$ , will enter the cavity and be reflected with a modulation of its phase and amplitude. The orthogonal polarization,  $|V\rangle$ , will simply be reflected by the first mirror of the cavity since the fraction going inside the cavity will be absorbed by the polarizer. The reflected light is then picked up and sent to a quarter waveplate and a polarizing beam splitter. The difference between the signals picked up at the two ports of the beam splitter creates the error signal.

Say the incoming light is linearly polarized with an angle  $\theta$  with respect to the linear polarizer inside the cavity. We call respectively  $A(\omega)$  and  $\phi(\omega)$  the amplitude and phase modulations of the reflected light with the parallel polarization. These modulations are the same as for a classic Fabry-Perot cavity and depend on the frequency of the laser  $\omega$ . We call  $r$  the reflectivity of the first mirror and  $E$  the amplitude of the field incident on the cavity's first mirror. The reflected light is  $E \left( A(\omega)e^{i\phi(\omega)} \cos \theta |H\rangle + r \sin \theta |V\rangle \right)$ . This light is then sent to a quarter wave plate whose fast axis forms an angle of  $\frac{\pi}{4}$  with  $|H\rangle$ . Thus,  $|H\rangle$  is transformed into  $e^{\frac{i\pi}{4}} |\sigma^+\rangle$ , and  $|V\rangle$  is sent to  $e^{\frac{3i\pi}{4}} |\sigma^-\rangle$ . The error signal obtained, sketched Figure 8a, is equal to:

$$\text{Err}(\omega) = |E|^2 r A(\omega) \sin(\theta) \cos(\theta) \sin(\phi(\omega))$$

This formula in itself is enough to understand that the polarizing beam splitter maps the phase difference and amplitudes of the two polarizations of the reflected light on the error signal.

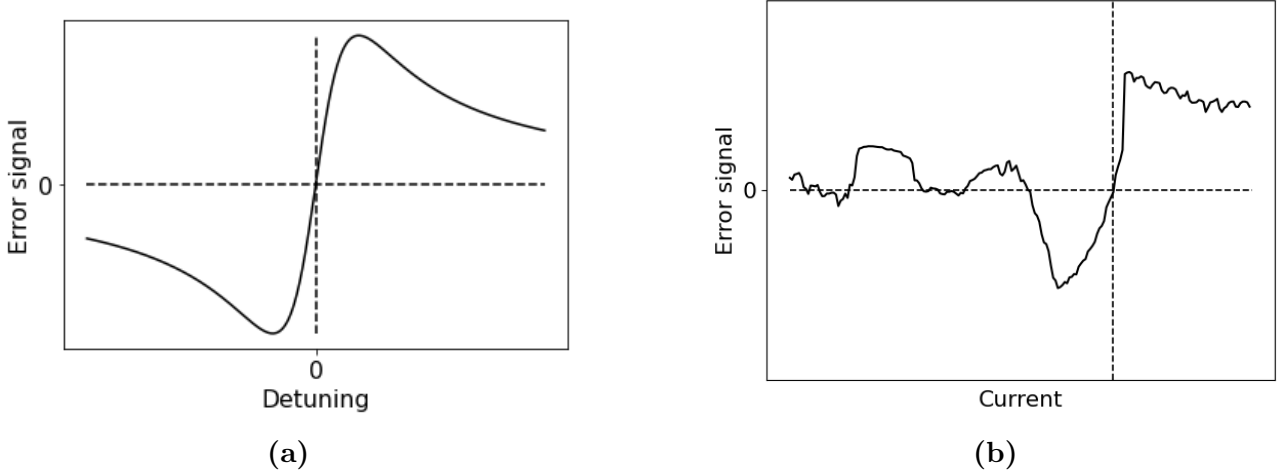


**Figure 8:** Figure 8a shows the theoretical error signal obtained using the Hänsch-Couillaud technique to lock the frequency of a laser on a cavity. Figure 8b shows an example of the error signal obtained using the Hänsch-Couillaud technique to lock the injection status of a laser diode.

A laser diode contains polarization-selective components that fix its output polarization. Hence, the two components of the PL's polarization will get different amplitude and phase modulation, which can be mapped to an error signal with a setup similar to the HC setup.

If  $A_H(I)$ ,  $A_V(I)$ ,  $\phi_H(I)$ , and  $\phi_V(I)$  are the amplitude and phase modulations of the two polarizations  $|H\rangle$  and  $|V\rangle$  after being reflected by the LD, then the error signal generated with the HC scheme is:

$$\text{Err}(I) = P_{seed} A_H(I) A_V(I) \sin(\theta) \cos(\theta) \sin(\phi_H(I) - \phi_V(I)) \quad (10)$$

$I$  is the current sent to the LD.

Figure 8b shows the error signal experimentally obtained. It is in appearance far from looking like Figure 8a. A further section of this thesis will be dedicated to understanding the different parts of this error signal from the physics of the injection-locking, but we first need to make sure that the unknown modulation of the orthogonal polarization ( $|V\rangle$ ) is not what gives the error signal this shape.

In principle, the effect of the LD's cavity on the parallel polarization ( $|H\rangle$ ) can be understood with Adler's equation for the injection, and the theory of Fabry-Perot cavities. However, it is harder to know how the orthogonal polarization ( $|V\rangle$ ) is modulated since we don't have access to the polarization-selective components inside the LD. Hence, we modified a bit the HC scheme to get information on the modulation of the orthogonal polarization. Figure 9 shows the basic HC setup (left-hand side setup). The polarization of the seed light is set to be linear with

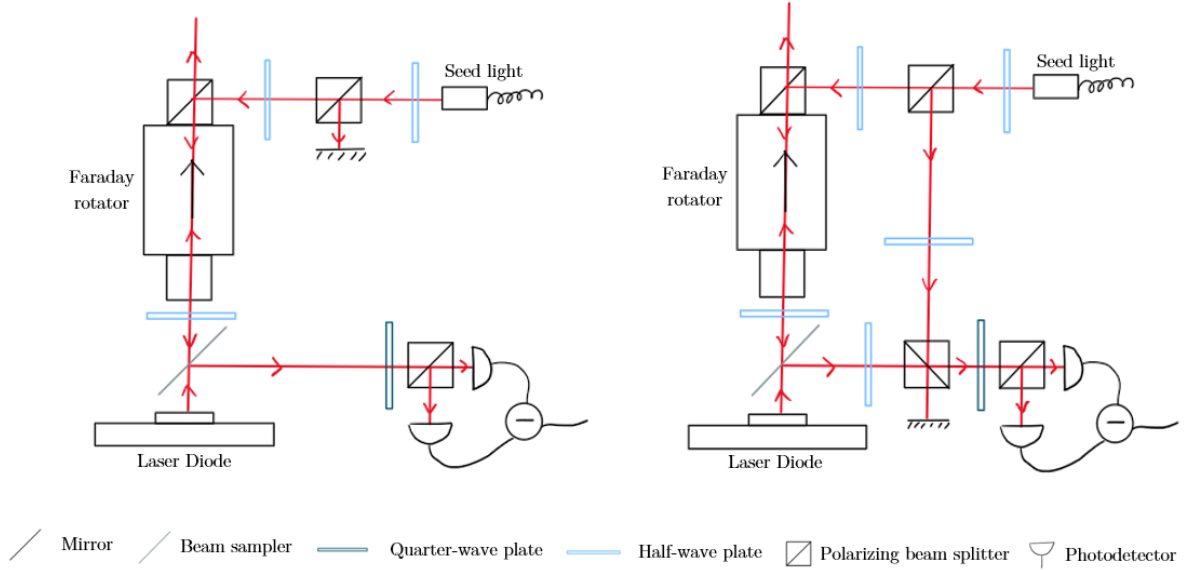


**Figure 9:** Diagrams of the optical setups used to generate the Hänsch-Couillaud error signal. When using the left-hand side optical setup, the seed light is linearly polarized with a non-null angle with respect to the natural polarization of the laser diode. It leads to a more stable error signal and is used to lock the injection status of the laser diode. When using the right-hand side optical setup, the seed light must have the same polarization as the free-running laser diode light. The error signal obtained is less stable due to the beam path difference between the two interfered beams.

an angle  $\theta$  with respect to the natural polarization of the LD. The reflected light is picked up with a beam sampler and sent to a quarter-wave plate, a polarizing beam splitter, and two photodiodes to generate the error signal described by (10).

The modified HC scheme is shown on the right-hand side of Figure 9. Instead of probing the phase shift acquired by the two polarizations when being reflected by the LD, we send the seed light with a polarization matching perfectly the natural polarization of the LD and mix this reflected light at a PBS with some previously picked-up seed light. The total light might carry an additional constant phase shift due to the different paths taken by the two beams, but the resulting signal should only carry information on the modulation of the parallel polarization. The error signal obtained should be equivalent to (10), but  $A_V(I)$  and  $\phi_V(I)$  now have constant values. When comparing the signals obtained with these two schemes, we saw no major difference, so we concluded that there is the equivalent of a linear polarizer inside the LD. Thus, we came back to the original and simpler scheme shown in Figure 9.

In the next section, we will show the full experimental setup. We will then try to understand why Figure 8b is different from the expected error signal depicted in Figure 8a.

II.3.2 • EXPERIMENTAL SETUP

Figure 10 shows a diagram of the full setup.

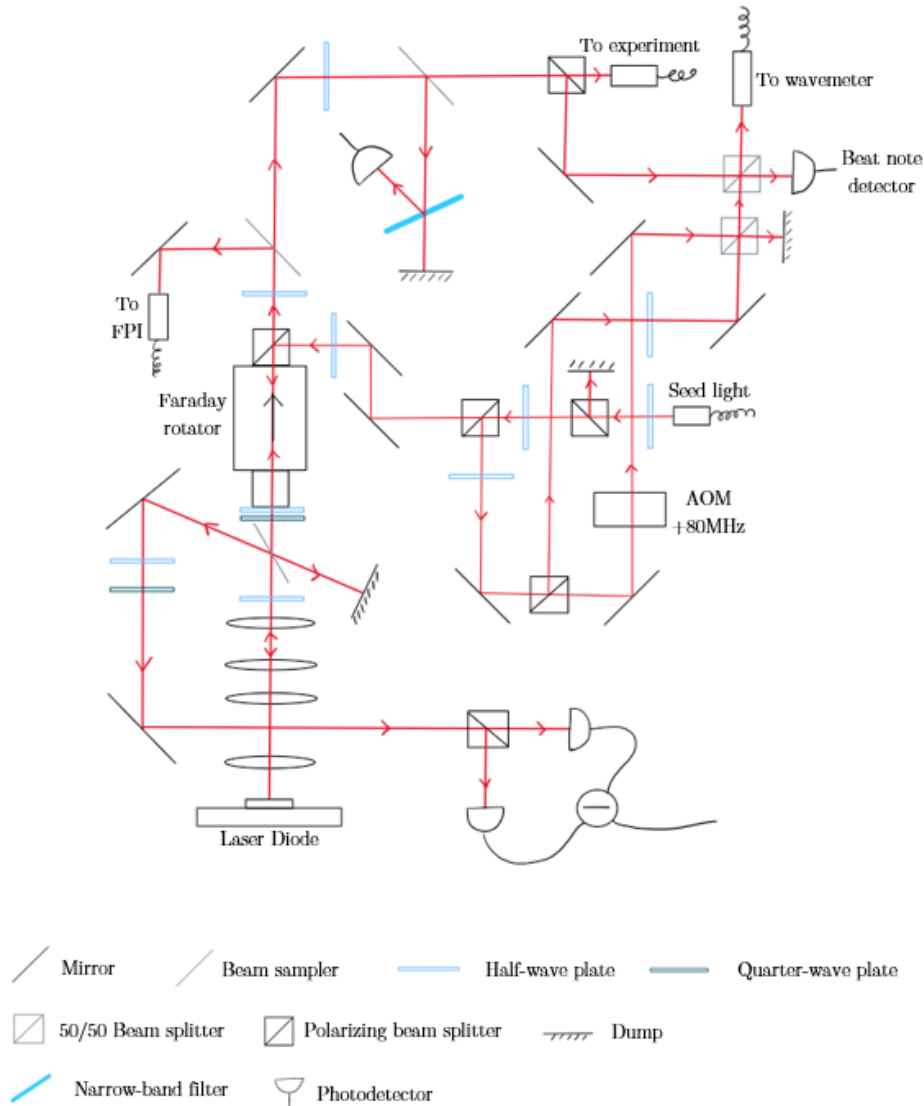


**Figure 10:** Diagram of the full optical setup built during the semester project. It allows to monitor the signal from the Fabry-Perot Interferometer and the error signals obtained with the Hänsch-Couillaud technique and the narrow-band filter. The light from the primary laser and the laser diode are sent to a wavemeter to monitor precisely their frequency. A beat note detector is built by shifting the frequency of the primary laser by 80 MHz. This frequency-shifted light is sent to a high bandwidth photodetector along with the initial primary laser light and light from the laser diode. Blocking one of the three beams allows to monitor the beat note signals between the two others.

To pick up the light reflected on the LD and generate the HC error signal, the uncoated face of a beam sampler is used at Brewster’s angle, combined with a half-wave plate. The reflectivity

## II. ACTIVE STABILIZATION OF THE INJECTION

of the beam sampler at Brewster's angle is very dependent on the polarization of the incident light. Hence, with the half-wave plate, we reduced the reflectivity of the  $|H\rangle$  polarization since it is the light that will be ultimately used for the experiment, and we want it to be mostly transmitted and not lost in the stabilization scheme. On the other hand, we increased the reflectivity of the  $|V\rangle$  polarization to have a larger error signal. The second half-wave plate after the beam sampler, along with the quarter-wave plate is used to maximize the transmission of the LD light through the Faraday isolator. The three waveplates around the beam sampler can be thought of as bridges between the polarizations required by the Faraday isolator (we want maximum transmission), by the beam sampler (we want only a small fraction of the  $|H\rangle$  light to be reflected), and by the LD (we want the light to be mostly linearly polarized along  $|H\rangle$ , with enough  $|V\rangle$  polarization to generate an error signal). We did not spend much time finding the optimum settings for the waveplates, ie the optimum ratios of the two polarizations  $|H\rangle$  and  $|V\rangle$  at the beam sampler and the LD, since they depend a lot on the seed power, and on the power needed by the photodiode to generate an error signal with a good signal-to-noise ratio.

The beam sampler at Brewster's angle helps reduce the losses of the amplified light in the error signal generation process, without reducing significantly the intensity of the error signal. However, the mirrors can add a phase shift between the two polarizations of the light when not used with a  $45^\circ$  incident angle. Since our error signal mainly relies on this phase shift, we used both a quarter and a half-wave plate before the PBS to have full control over the polarization of the light and so on the error signal.

Furthermore, as discussed in the previous section, a good feature of the HC error signal that we intend to keep is that it is equal to 0 at the targetted injection current. This relies on the assumption that the phase shift  $\phi(I)$  is also equal to 0 at the best injection setting. From equation (7), we learned that in a semiconductor LD, the injected LD light gets a phase shift  $\psi = -\arctan(\alpha)$  in addition to the phase shift inherent to the injection-locking mechanism. In order to still get a null error signal at the optimum injection current, we set the half and quarter wave plate to send the  $|H\rangle$  polarization to  $\frac{1}{\sqrt{2}}(|H\rangle + e^{i\beta}|V\rangle)$  instead of  $|\sigma^+\rangle$ . The generated error signal will then be (up to a proportionality constant):

$$\text{Err}(I) = P_{seed} A_H(I) \sin(\theta) \cos(\theta) \sin(\phi_H(I) - \beta') \quad (11)$$

This  $\beta'$  can be given any value with the waveplates to compensate for the phase shifts acquired due to the injection or the reflection at the beam sampler. When carefully set, the waveplates allow to get an error signal equal to 0 and linear at the injection current, for any seed power. That is a huge advantage over the two locking techniques presented so far since the feedback loop will be robust against power fluctuations.

Figure 11 shows a compilation of error signals obtained for different waveplates settings. In Figures 11a, 11b, and 11c, we changed the value of the phase shift  $\beta$  between  $|H\rangle$ , and  $|V\rangle$ . The red part of the error signal shows the currents at which clean injection is obtained (monitored with a wavemeter). The signal can be given any shape between rather linear and rather flat. We understand it as  $\phi_H(I)$  being rather linear within the clean injection range, and the phase shift  $\beta'$  showing different parts of the sinus function (see Equation (11)). For instance, we can roughly estimate that  $\beta' = 0$  in Figure 11a,  $\beta' = \frac{\pi}{2}$  in Figure 11b, and  $\beta' = \frac{3\pi}{4}$  in Figure 11c.

To obtain Figures 11d, 11e, and 11f, we tuned the waveplates such that the error signal is equal to 0 at a clean injection current for any seed power.

In the end, keeping track of the phase shift acquired by the two polarizations at the LD or the beam sampler is not realistic. Thus, we mostly tuned the waveplates by looking at the error signal and trying to optimize its shape within the clean injection region.

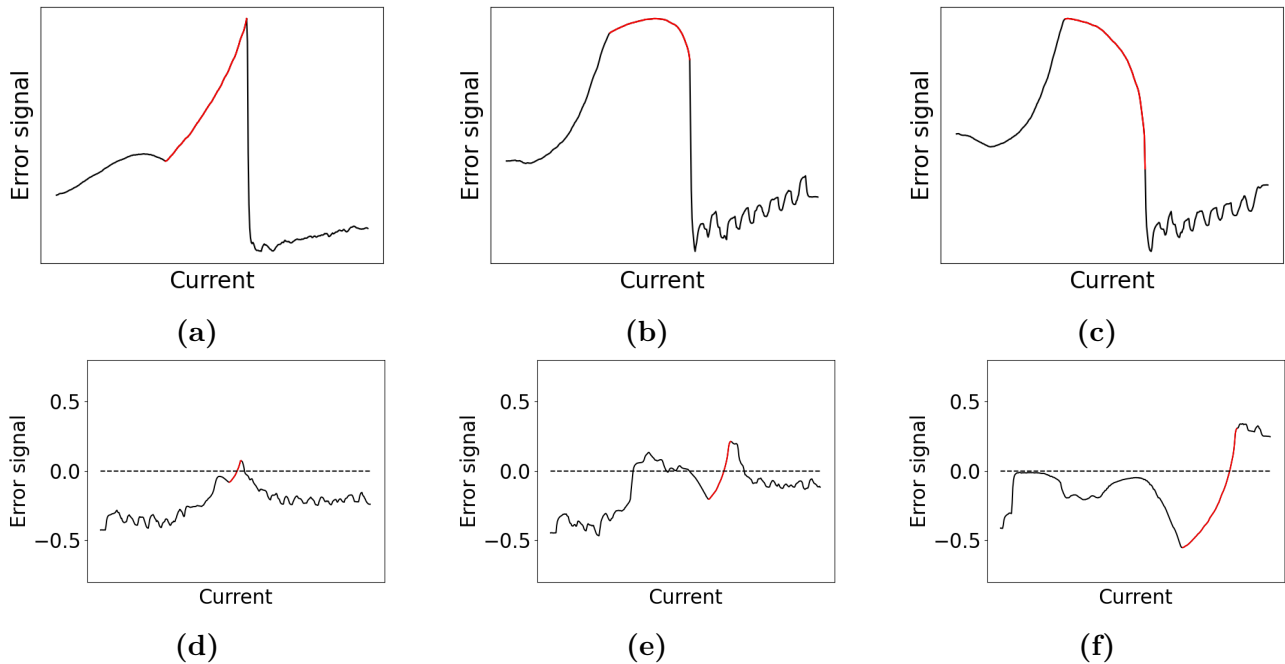


**Figure 11:** Hänsch-Couillaud error signal obtained for many different settings of waveplates. The red part of the error signal always shows the current at which clean injection is obtained (monitored with a wavemeter). Figures 11a, 11b, and 11c show the error signals obtained with the same seed power but different waveplates settings. Figures 11d, 11e, and 11f show the error signals obtained with different seed powers ( $60 \mu\text{W}$ ,  $150 \mu\text{W}$ , and  $400 \mu\text{W}$  respectively) when the waveplates are correctly tuned.

We also sent the LD light to an FPI setup, and to the carefully oriented narrow-band filter to compare the three different error signals. This was useful when trying to understand the behavior of the LD close to the injection since all these signals convey different information. A wavemeter picking up light from the PL and the LD was also used to complete these pieces of information.

The Acoustico-Optical Modulator (AOM) and the beat note detector will be used further to analyze the noise added to the injected LD light.

## II.3.3 • UNDERSTANDING THE OBTAINED ERROR SIGNAL:

In order to understand the physics behind the error signal shown in Figure 8a, we monitored at the same time the three error signals that we already presented: the transmission of the FPI, the reflection on the narrow-band filter, and the HC error signal. We also used the wavemeter to know more precisely the frequency of the main mode in the output of the laser diode.

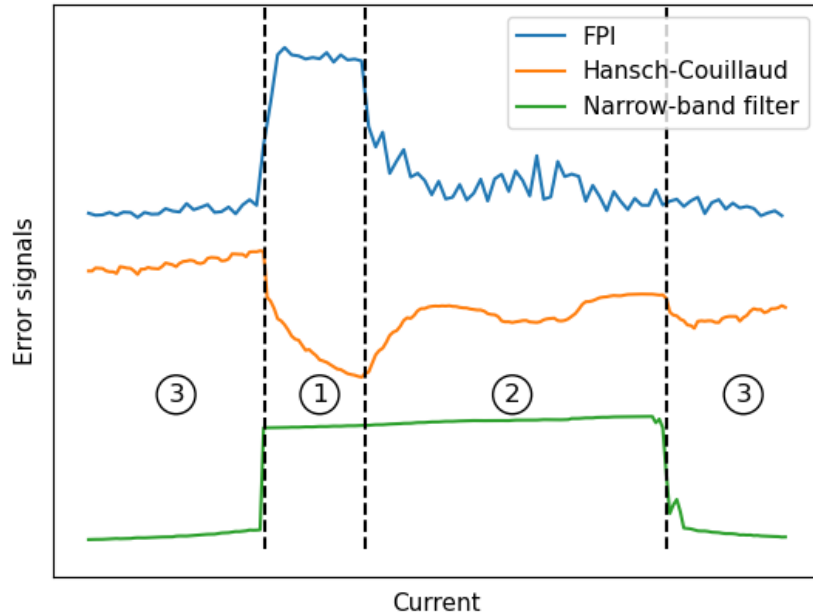


**Figure 12:** Comparison between three error signals: the transmission through the Fabry-Perot Interferometer (FPI), the Hänsch-Couillaud error signal, and the power of the light reflected off the narrow-band filter. The numbers indicate the three injection regimes: 1 for the clean injection regime, 2 for the bad injection regime, and 3 for the free-running mode.

Figure 12 shows the three error signals measured at the same time, while scanning the current around an injection current. The scales and offsets of the three error signals have been changed for better readability.

Also, like in Figure 7, the numbers indicate the injection regime.

Number 1 indicates the clean injection regime: the transmission through the FPI is maximum, as for the intensity of the light reflected on the narrow-band filter. The wavemeter shows that the light runs single-mode at the exact same frequency as the PL.

Number 2 indicates the bad injection regime: the transmission through the FPI is decreased, and new modes appear in the spectrum of injected LD light. The frequency measured by the wavemeter is very close to PL frequency, but not equal, and continuously varies with the current within region 2. The light is still reflected by the narrow-band filter since the frequency of the light is still close to the PL frequency.

Number 3 indicates no injection and free-running operation of the LD: the transmission through the FPI is very weak, as for the signal measured at the reflection of the narrow-band filter.

## II. ACTIVE STABILIZATION OF THE INJECTION

When it comes to the HC error signal, we see different behaviors in these three regimes. What interests us is that it is indeed quite linear and equal to 0 (not shown in this graph) in the clean injection regime. In addition, it behaves differently enough in the other regimes to know from the HC error signal alone where the clean injection takes place.

Hence, this error signal has all the features required to be used with a feedback loop and stabilize the injection status of the LD. Furthermore, the HC error signal has sharp edges at the two borders of the clean injection regime, which makes it a precise and reproducible metric to measure the injection range. We will use it throughout all section 3 to measure the injection range, and so the passive stability of the injection.

### II.4 OPTIMIZING THE FEEDBACK LOOP

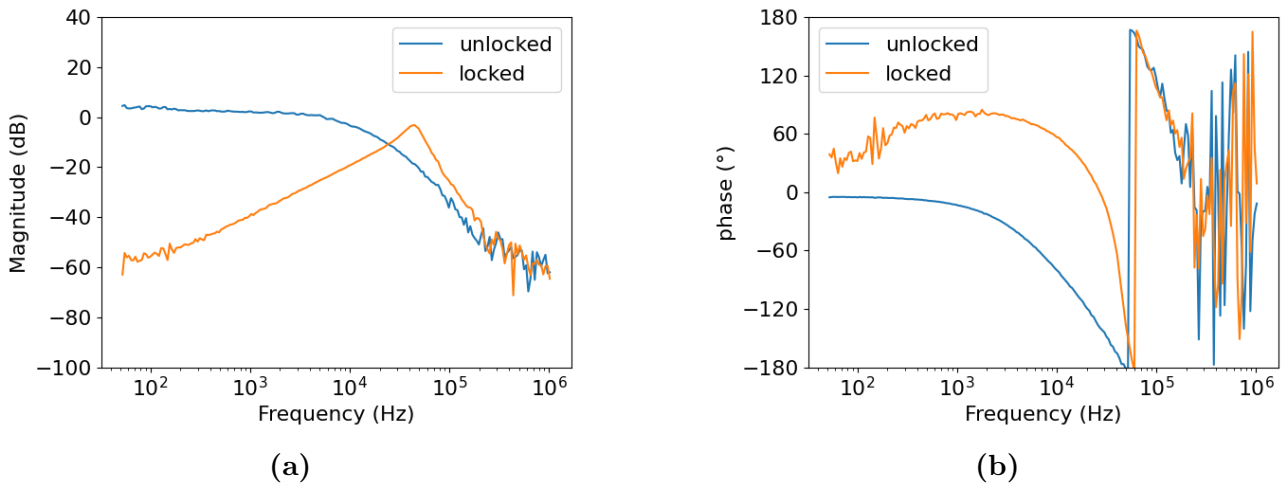


**Figure 13:** Bode plots of the transfer function of the feedback loop while the injection is locked or unlocked. When locked, the Bode plot shows the disturbance attenuation of the feedback loop. Figure 13a shows the magnitude of the transfer function while Figure 13b shows its phase.

Before feeding it back to the current controller to stabilize the injection, the error signal needs to be modified with a PI controller to fit better the system's characteristics. The PI controller will apply the transfer function  $H(s) = K(1 + \frac{\omega_{PI}}{s})$  to the error signal.  $K$  is the gain, and  $\omega_{PI}$  is the P-I corner of the feedback loop. Setting correctly the two parameters  $K$  and  $\omega_{PI}$  can be done by measuring the characteristics of the system. To do so, we measured the transfer function of the full system using the "Analog discovery 2". This device automatically sends a sinusoidal signal of different frequencies to the current controller of the LD and measures the phase shift and change of amplitude in the sinusoidal response of the system (the error signal). This needs to be done with a sinusoidal amplitude lower than the injection range such that the error signal is linear over the sinusoidal scan sent by the Analog discovery 2.

## II. ACTIVE STABILIZATION OF THE INJECTION

Thus, we increased the seed power to 1.5 mW for this measurement. The Bode plots of the transfer function are shown in Figure 13. We showed the transfer functions for the unlocked system and the measured disturbance attenuation of the feedback loop after we optimized the feedback loop settings. The comparison between the two shows the effect of the feedback loop. In Figure 13a, we show the magnitude of the transfer function of the system. The observed bandwidth of the unlocked system is around 30 kHz. In Figure 13b, we observe a  $180^\circ$  phase shift in the sinusoidal response of the unlocked system around 50 kHz. The choice of the P-I corner frequency depends on a lot of parameters and would need some time and thinking to be decided. However, it was not the goal of the semester project to optimize this part of the loop. Thus, we simply set the P-I corner to 30 kHz to roughly match the system's bandwidth and be lower than the frequency at which a  $180^\circ$  phase shift is observed to avoid servo bumps. The choice of the gain  $K$  depends entirely on the slope of the linear error signal obtained, which is dependent on the waveplates and the seed power. Hence, there is no fixed value for this gain, but the strategy to lock is generally to start with no gain, lock the injection, and slowly increase  $K$  until oscillations are observed in the error signal.  $K$  is then slightly decreased from the value at which oscillations are observed. In Figure 13a we observe that the magnitude of the transfer function of the system when locked with the feedback loop changes a lot. The magnitude of the transfer function is decreased by the feedback loop, which indicates that the loop effectively suppresses noise at frequencies below the P-I corner.

By optimizing the feedback loop settings, we managed to stabilize the injection lock with only  $20 \mu\text{W}$  of seed power and 35 mW of output power for a few hours. With this little seed power, the injection locking is only stable for a few minutes if we don't actively stabilize the current (the current controller used is quite noisy). Hence, in this small seed power regime, there is a clear improvement by one or two orders of magnitude in the stability of the injection locking thanks to the feedback loop. When the seed power is larger, above  $200 \mu\text{W}$ , the injection range is large enough for the injection locking to be passively stable for a few days. Hence, it is hard to compare the stability with and without a feedback loop since it would require not working on the setup for a week. However, in a realistic operation of the injection locking, we would like to amplify light transmitted through a high finesse cavity, whose power is lower than  $50 \mu\text{W}$ . In this range of seed power, the feedback loop does help with the stability of the current.

# III

## INCREASING THE PASSIVE STABILITY OF THE INJECTION-LOCKING

---

### III.1 INJECTION RANGE VERSUS SEED POWER AND OUTPUT POWER OF THE DIODE

---

We have already derived a theoretical injection range  $\Delta\omega = \frac{1}{2\tau_{inj}} \frac{|A_1|}{|A_0|} \sqrt{1 + \alpha^2}$ . This formula indicates that the injection range is proportional to the square root of the seed power, and inversely proportional to the square root of the circulating power, and so to the output power of the LD.

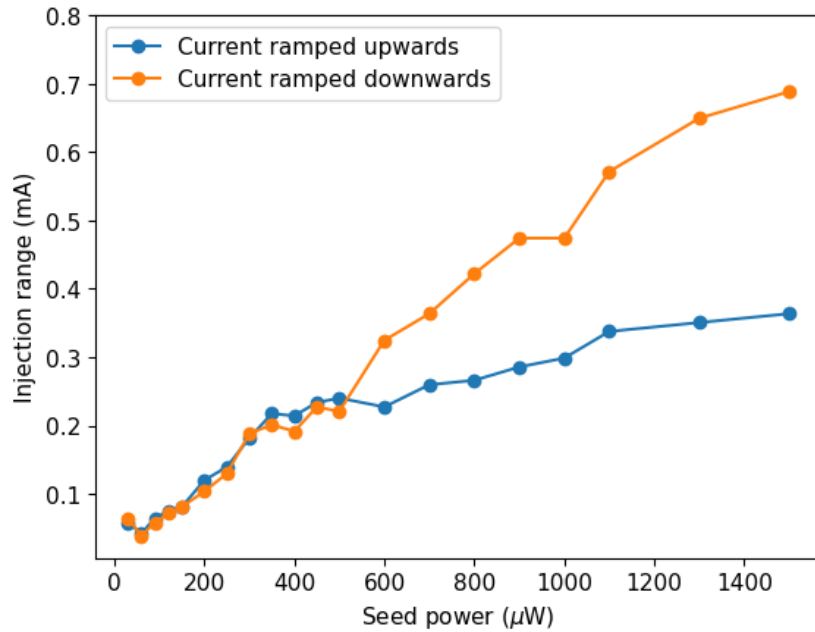
#### III.1.1 • INJECTION RANGE VERSUS SEED POWER

Figure 14 shows the measured injection range for different seed powers. We have already discussed the hysteresis behavior of the injection due to the influence of the circulating power on the effective length of the LD's cavity. The two traces in Figure 14 show that the injection range measured with the HC error signal indeed changes whether one scans the current upwards or downwards. However, this difference in injection range is mostly due to an overshooting of the length of the cavity when arriving at resonance. Indeed, the sudden increase of circulating power increases the length of the cavity, driving it off-resonance. Therefore, once the current is tuned to an injection point, the true injection range, defined by how much the current can be changed until the injection is lost, should not be dependent on whether the injection current was reached from higher or lower currents. Thus, in the rest of this thesis, we only measured the injection range based on the HC error signal when the current has been scanned downwards.

As expected, the injection range measured increases with the seed power. Nevertheless, we don't observe the 'square root' behavior predicted by the formula. We don't know if it is due to our measurement not being precise enough, or to the injection range formula being based on a 'too simple' model of the semiconductor laser diode.

#### III.1.2 • INJECTION RANGE VERSUS OUTPUT POWER

The measurement of the injection range for different output powers is slightly more subtle. Changing the output power of the LD is done by changing the current. However, changing the current sent to the LD drives it out of the clean injection regime. Thus, we also had to change



**Figure 14:** Evolution of the clean injection range with the seed power. This injection range is measured from the Hänsch-Couillaud error signal. To get both traces, we either monitored the injection range by ramping the current upwards throughout the injection regime, or downwards. The difference between the two traces comes from the hysteresis phenomenon explained in the text.

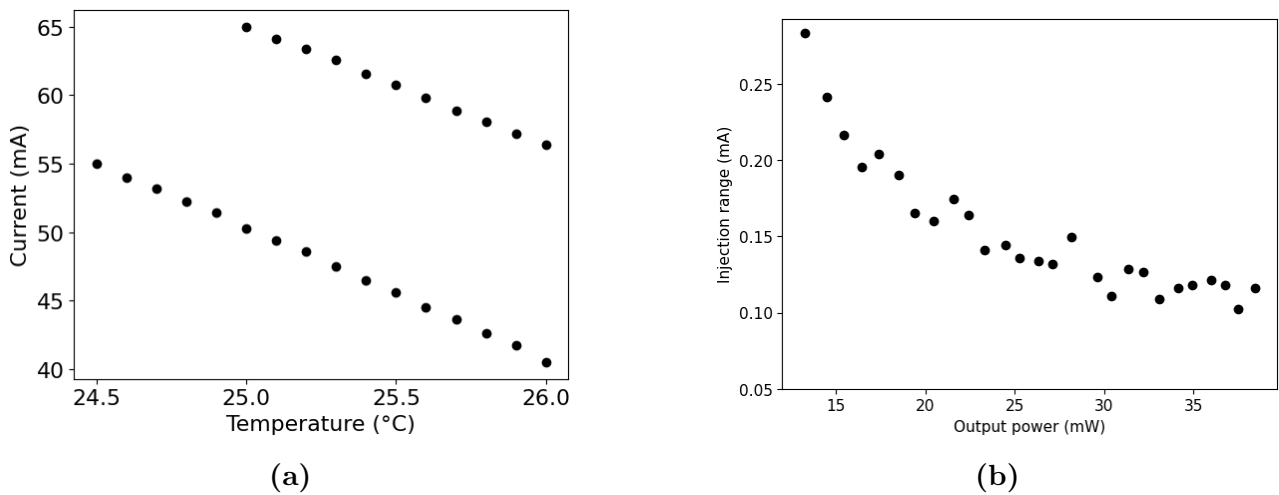


**Figure 15:** Figure 15a shows the injection points used to measure how the injection range changes with the output power of the laser diode. Figure 15b shows the result of this measurement.

the temperature to change the mean current of clean injection, and so the mean output power, as shown in Figure 15a.

The measurement was done by fixing the seed power to  $P_{seed} = 235 \mu W$  and changing the temperature over a range as small as possible to minimize its potential influence on the injection range. Figure 15a shows the set of injection points used for the measurement. Each point corresponds to a different current of injection, which can then be mapped to an output power using Figure 2a. The result of the measurement is shown in Figure 15b.

As described by the theory, the injection range decreases with the output power of the LD. There is a clear trade-off between a good amplification of the seed light and a good stability of the injection.

## III.2 INFLUENCE OF THE TEMPERATURE

A modification of the temperature of the LD has many effects. First, the refractive index of the p-n junction can be changed, as well as its gain spectrum. In addition, the relative position of the two mirrors forming the Fabry-Perot cavity can be changed. This can have an impact on the length of the cavity, and so on its resonance frequencies. It can also change the modes of the cavity, and so the output beam's profile and direction of propagation. These two parameters are non-negligible since their modification leads to a lower coupling of the seed light into the LD's cavity. Hence, we decided to first investigate how much the direction of propagation of the LD beam was changed with the temperature before investigating the effect of the shift of the gain spectrum of the LD.

### III.2.1 • INFLUENCE OF THE TEMPERATURE ON THE BEAM PROFILE AND DIRECTION OF PROPAGATION

There is no direct way of measuring how much seed light is coupled into the LD's cavity. Thus, we decided instead to measure how much of the LD light was coupled into the fiber that brings the seed light to the optical table.

We started by optimizing the fiber coupling at a fixed temperature (25 °C). Then, we changed the temperature without re-aligning the beams and measured the fiber coupling obtained. Figure 16a shows the result of the measurement. We observe a quite large modification of the fiber coupling with the temperature (around 10% every 1.5 °C), which we interpret as a modification of the direction of propagation of the LD beam. In principle, modifying the fiber coupling changes the effective seed power, which, as shown in Figure 14, has a large influence on the injection range. Figure 16b shows how the beam matching between the PL and LD, quantitatively described by this fiber coupling, changes the injection range. This measurement was done by fixing the temperature and misaligning the optics to decrease the fiber coupling. The injection range was once again measured from the HC error signal.

The modification of the LD beam's direction of propagation is something to have in mind when doing measurements where the temperature is changed, but it can be compensated by re-aligning the optics. However, if the beam profile or collimation is changed with the temperature, one would need to change the lens system to compensate for it, which would take much more time than a slight re-alignment of mirrors. We measured in Figure 16c the maximum fiber coupling obtained for each temperature. The graph obtained not being constant means that the beam profile does change with the temperature. The 'optimum temperature' that maximizes the fiber coupling is not an absolute value but is dependent on the lens system built. Hence, one must take care of aligning the lens system only after the temperature of the LD has been set to its permanent value. With our lens system, the injection locking is likely to be more stable around 28 °C rather than around 22 °C.

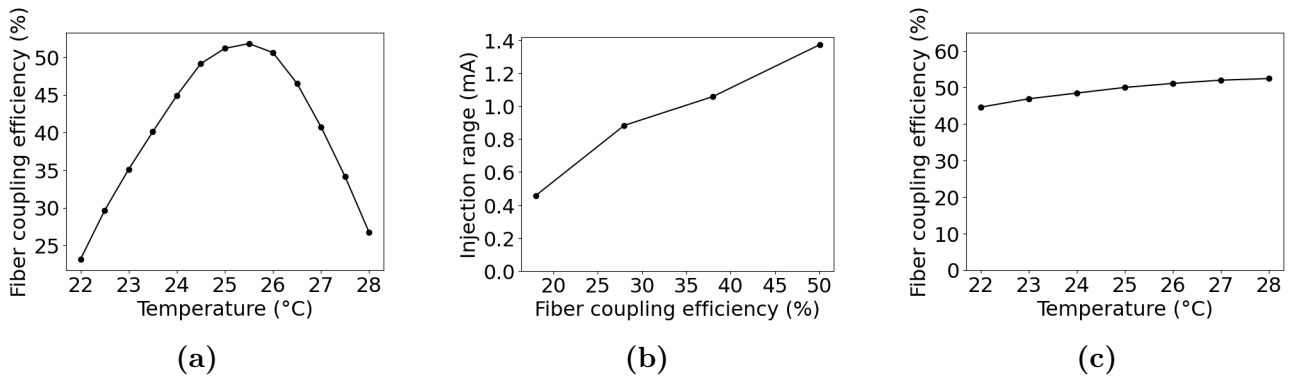


**Figure 16:** Figure 16a shows how much the laser diode beam direction of propagation is changed when the temperature of the laser diode is modified. The beam was first coupled to a fiber at 25 °C, then the temperature was changed and the fiber coupling was monitored without recoupling throughout the measurement. Figure 16b shows the injection range as a function of the coupling of the laser diode light to the fiber bringing the seed light to the optical table. Figure 16c shows the maximum fiber coupling of the laser diode as a function of its temperature

### III.2.2 • INFLUENCE OF THE TEMPERATURE ON THE GAIN SPECTRUM

We have already shown with Figure 2b that the free-running wavelength of the LD changes with the temperature. This could have an impact on the competition between the free-running mode and the injected mode of the LD, and so an impact on the clean injection range.

Thus, we measured the clean injection range for different seed powers at two very different temperatures: 24.80 °C (the free-running wavelength of the LD is 1.5 nm away from the PL wavelength), and 33.90 °C (the free-running wavelength of the LD is very close to the PL wavelength). We have already seen that many parameters have an impact on the injection range. Hence, in order to make sure that our measurement of the clean injection range would only show the impact of the detuning between the free-running and PL frequencies, we made sure to have the exact same output power of the LD and mode matching between the PL

and LD beams throughout the measurement. The output power was chosen to be 30 mW because, as shown in Figure 15b, a measurement imprecision on the output power leads to less imprecision on the clean injection range at higher output powers. Figure 17 shows the result of the measurement of the clean injection range at different seed powers. Figure 17b is a zoom-in of Figure 17a on the lower seed powers. For most seed powers, we observe no major

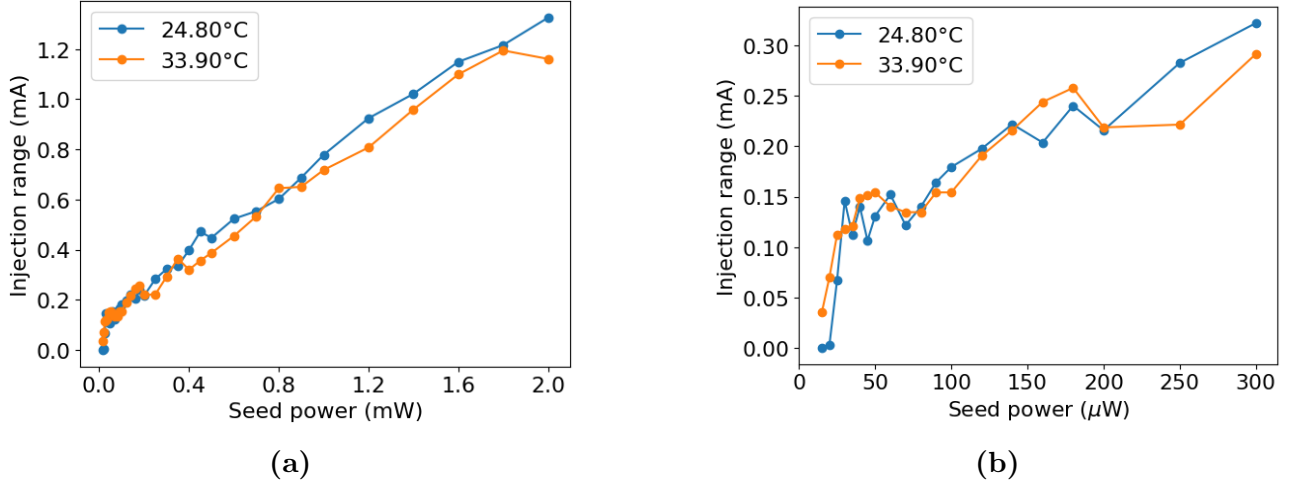


**Figure 17:** Clean injection range measured for different seed powers at 24.80 °C and 33.90 °C. Figure 17a shows the full measurement for seed powers between 0 and 2 mW. Figure 17b is a zoom-in of Figure 17a, showing the measured clean injection ranges for seed powers between 0 and 300  $\mu$ W

difference between the clean injection range at these two temperatures. However, we observed that the LD was never entirely injection-locked below 20  $\mu$ W at 24.80 °C, whereas it could be injection-locked at 33.90 °C with only 15  $\mu$ W of seed power. This lower minimum seed power required for injection-locking at 33.90 °C results from the mode competition between the injected mode and the free-running mode of the LD. Figure 18 shows a physical picture of the unsaturated gain and gain threshold of the laser diode at two different temperatures. At 24.80 °C, the free-running frequency  $\omega_{FR}$  is far from the seed light frequency  $\omega_1$ . Hence, the unsaturated gain of the Fabry-Perot mode around the frequency  $\omega_1$  is rather small and the seed power needed to reach the gain threshold, and to injection-lock the LD is high. At 33.90 °C, the two frequencies are closer and have similar unsaturated gains. Hence, the seed power needed for the injection-lock mode to win the mode competition against the free-running mode of the LD is smaller.

At higher seed powers, the injection range is no longer limited by the mode competition between the free-running and injected modes, but rather by the steady-state solution constraint of Adler's equation (see equation (5)). Hence, the injection ranges at 33.90 °C and 24.80 °C are very similar.

Finally, this shows that the optimum operating temperature of the LD depends a lot on the seed power. In the small seed power regime, running the LD around 34 °C leads to better passive stability. Nevertheless, in the large seed power regime, the temperature does not change

dramatically the injection range. 25 °C may be a better operating temperature since it is closer to the lab's temperature and is recommended by the manufacturer for the longevity of the diode. In both cases, one must be careful of choosing this operating temperature before building the lens system, since the choice of lenses depends on LD's beam profile, and so on the temperature.

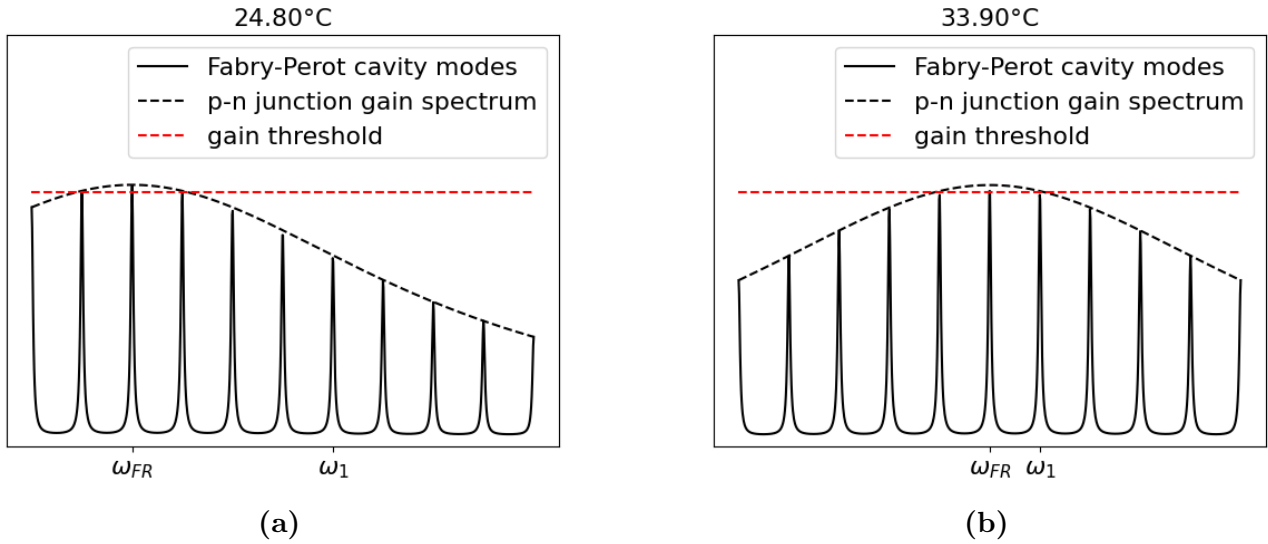


**Figure 18:** Physical picture of the laser diode's unsaturated gain spectrum (in black) and the gain threshold (in red) at two different temperatures 24.80 °C and 33.90 °C.  $\omega_{FR}$  refers to the free-running frequency while  $\omega_1$  refers to the seed light frequency

## IV SPECTRUM OF THE AMPLIFIED LIGHT

---

### IV.1 SETTING UP A BEAT NOTE SETUP

---

Now that we understand how to make the injection lock as stable as possible, it remains to make sure that the linewidth of the amplified light is the same as the primary laser's linewidth, and that no noise is added to the light through the LD.

In order to do so, we picked off some of the PL light and shifted its frequency by 80 MHz with an Acoustic Optical Modulator (AOM). We then overlapped this frequency-shifted beam with the initial PL beam and the output of the LD at a photodiode (see Figure 10). We could therefore measure the beat note signal between any two of these three beams by blocking the third. In theory, the spectrum of the injected light should be exactly the same as the spectrum of the PL. This should lead to the exact same beat note signal between the frequency-shifted PL and LD as between the original PL and the frequency-shifted PL.

### IV.2 BEAT NOTE SPECTRUMS

---

The injected light would ultimately be used on ions. The frequency of the noise that can reduce the most the quality of the operations performed on ions is in the 100 kHz to around 5 MHz range since it corresponds to the resonance frequency of the motion of the ions. Hence, we analyzed the spectrum of the beat note signal with a spectrum analyzer with both a 4 MHz and a 400 kHz frequency span around the center frequency 80 MHz.

#### IV.2.1 • BEAT NOTE SPECTRUMS OBTAINED WITH DIFFERENT CURRENT CONTROLLERS

Figure 19 shows the obtained beat note spectrums using two different current controllers (LDC240C and LDC202C from Thorlabs [3]). The seed light beat note signal refers to the beat note between the bare seed light and the frequency-shifted seed light. The injection beat note refers to the beat note signal between the output of the LD and the frequency-shifted seed light. Figures 19a and 19b show the first beat note signals obtained. We compared the injection beat note with the seed light beat note with and without the feedback loop to lock the current to see its influence. We observe that the noise figure of the injection beat note is much worse than that of the seed light beat note. The current controller we used for this measurement (LDC240C) is capable of sending currents from 0 to 4 A, whereas we only need

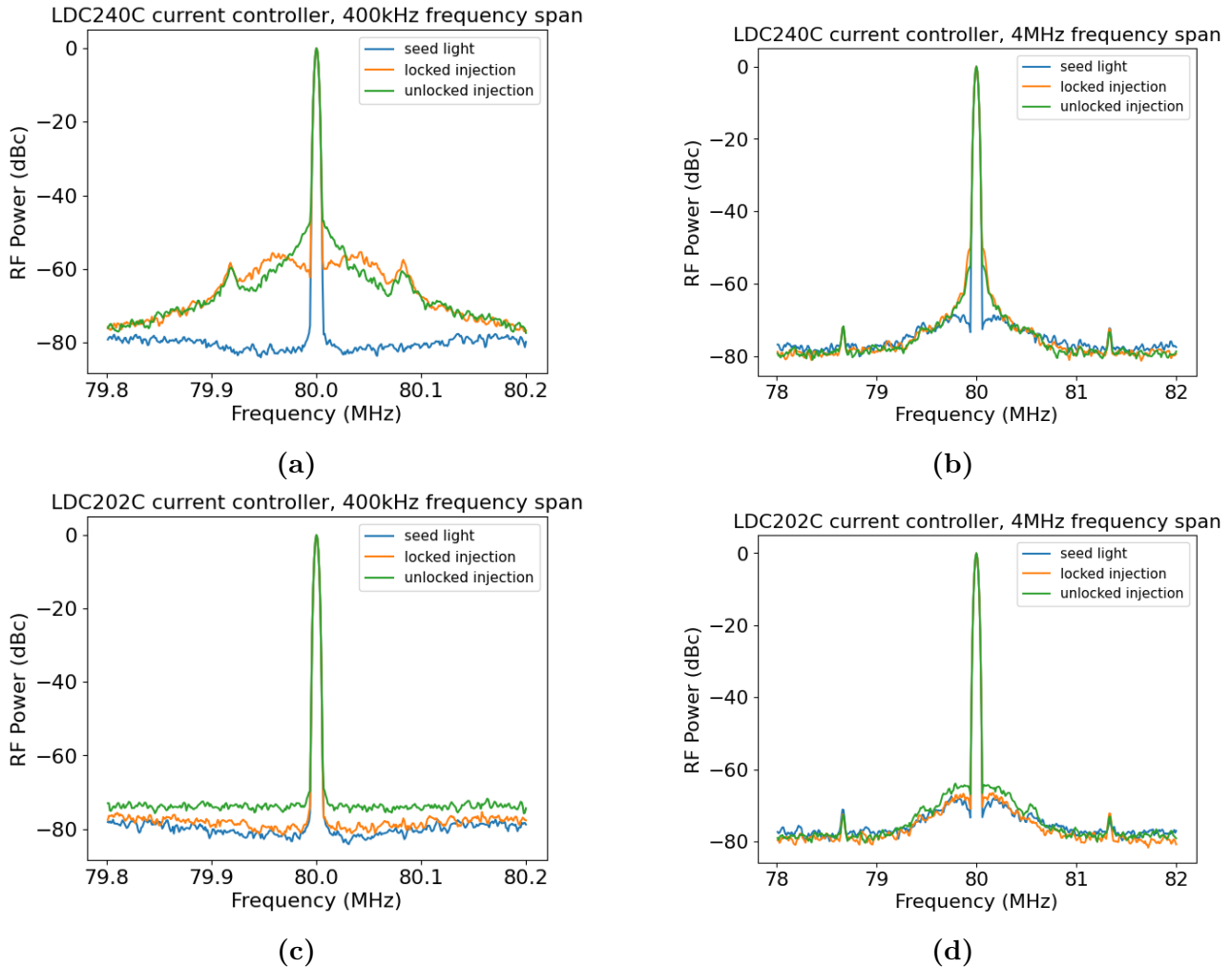


**Figure 19:** Comparison of different beat note spectrums between the frequency-shifted seed light and the bare seed light, or between the frequency-shifted seed light and the injected laser diode light. Figure 19a and 19b show the beat note spectrums obtained with the current controller LDC240C from Thorlabs at two different frequency spans. The injected laser diode beat note is shown with and without locking the current with a feedback loop. Figure 19c and 19d show the same beat note spectrums with the current controller LDC202C from Thorlabs.

less than 70 mA to control our LD. Since this current controller is certainly not designed for the small currents we operate at, we switched to another current controller (LDC202C) whose current ranges from 0 to 200 mA. Figures 19c and 19d show the obtained beat note signals. We observe a net improvement in the noise figure if we compare the injection and seed light beat notes. Furthermore, we observe that locking the current of the LD reduces a bit the noise in the injected light. This second controller has a better-suited current range, but it is of the same brand (Thorlabs), and might still bring some noise to the injected light, a more precise controller might be able to reduce the noise even further. Unfortunately, a better controller was ordered but did not arrive before the end of the project.

## IV.2.2 • OTHER BEAT NOTE SPECTRUMS

In Figure 20a, we compare the beat note signals obtained with different values of the gain  $K$  of the feedback loop. As expected, higher gain means better suppression of the noise within the loop bandwidth (30 kHz) but generates servo bumps around 60 kHz.

Finally, Figure 20b compares the beat note spectrum when injecting at different values of the current (and so output power of the diode). We observe that the lower the output power of the diode, the lower the noise. Since the three spectrums have been measured with the same seed power, this better noise figure is understood as a consequence of the larger injection range at lower currents.

In addition, we measured the beat note signal obtained at different temperatures of the LD but obtained similar beat note signals and concluded that the temperature of the LD has no, or small, impact on the noise added to the light through the injection locking.

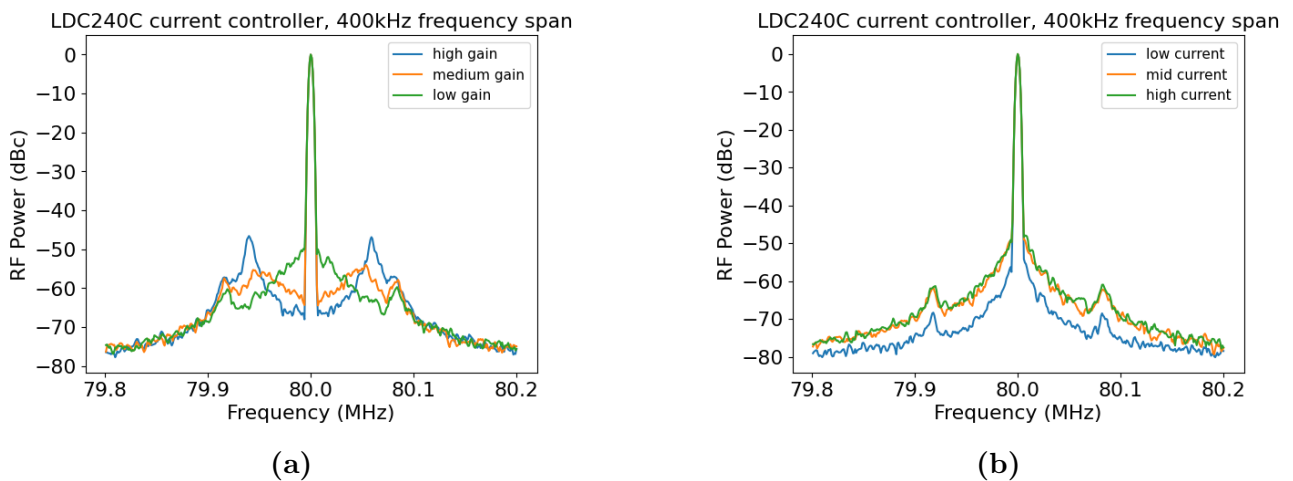


**Figure 20:** Figure 20a shows the beat note spectrum between the frequency-shifted seed light and the injected laser diode light whose current is locked with different gains. Figure 20b shows the beat note spectrum between the frequency-shifted seed light and the unlocked injected laser diode light at different currents of injection.

# V

## CONCLUSION

---

The main outcome of this Semester project was the adaptation of the Hänsch-Couillaud stabilization scheme on the injection locking of a semiconductor laser diode. It not only allows to efficiently stabilize the frequency difference between the primary and secondary lasers for almost free (it requires only a few basic optics components) but the error signal generated was found to be an excellent metric for the clean injection range. The latter outcome allowed us in this thesis to characterize with precision the passive stability of the injection-locking and how the different physical parameters modify this passive stability. The influence of the seed and output power on the passive stability was discussed, as well as the influence of the mode-matching between primary and secondary lasers and the temperature. Furthermore, we observed a net improvement in the duration of the injection locking when using the error signal to actively stabilize the current in the small seed power regime (from a few minutes to a few hours with  $20 \mu W$  of seed power).

All this work has been done on a temporary setup, using a tunable seed light to study the injection locking in more detail. Some mistakes have been made while building this setup, like a bad choice of current controller and breadboard to protect the system against external noise. We hope that this work serves as a tool on how to build a better permanent setup

# VI ACKNOWLEDGEMENTS

---

I would like to thank Julian Schmidt, Luka Milanovic, and Robin Oswald for their supervision and help throughout this project. I learned a lot from their shared experience and wouldn't have been able to go this far without their support.

I would also like to thank Jolan Tissier for his communicative joy. He made working in the lab on a Friday afternoon much funnier.

Lastly, I would like to thank Dr. Cornelius Hempel and Prof. Jonathan Home for giving me the opportunity to work in the Ion Trap Quantum Computing group on such an interesting project.

## BIBLIOGRAPHY

---

- [1] A. Aspect et al. *Optique quantique 1, Photons et Atomes*. 2021.
- [2] F. Mogensen, H. Olesen, and G. Jacobsen. “Locking Conditions and Stability Properties for a Semiconductor Laser with External Light Injection”. In: *IEEE Journal of Quantum Electronics* (1985).
- [3] Thorlabs. URL: [https://www.thorlabs.de/navigation.cfm?guide\\_id=1](https://www.thorlabs.de/navigation.cfm?guide_id=1).
- [4] Roxana Wedowski. *Injection locking of lithium diodes*. 2021.
- [5] B. Saxberg, B. Plotkin-Swing, and S. Gupta. “Active Stabilization of a Diode Laser Injection Lock”. In: *Review of scientific instruments* (2016). DOI: 10.1063/1.4953589.
- [6] R. Oswald. “Characterization and control of a cryogenic ion trap apparatus and laser systems for quantum computing”. PhD thesis. 2022.
- [7] E. D. Black. “An introduction to Pound–Drever–Hall laser frequency stabilization”. In: *American Journal of Physics* (2001).
- [8] Z. Chen et al. “Active control of a diode laser with injection locking”. In: *Review of scientific instruments* (2021). DOI: 10.1063/5.0057245.
- [9] G. Mueller and K.-I. Ueda. “Stabilization of Injection Locking using Polarization Spectroscopic Technique”. In: *Japanese journal of applied physics* (1998). DOI: 10.1109/3.918577.
- [10] U. Mishra et al. “Monitoring and active stabilization of laser injection locking using beam ellipticity”. In: *Optica* (2023). DOI: 10.1364/OL.495553.
- [11] R. D. Niederriter, I. Marques Van Der Put, and P. Hamilton. “Polarization purity for active stabilization of diode laser injection lock”. In: *Review of scientific instruments* (2021). DOI: 10.1063/5.0059824.
- [12] D. J. Ottaway et al. “Stabilization of Injection-Locked Lasers Using Spatial Mode Interference”. In: *IEEE Journal of quantum electronics* (2001). DOI: 10.1109/3.918577.
- [13] T.W. Hansch and B. Couillaud. “Laser frequency stabilization by polarization spectroscopy of a reflecting reference cavity”. In: *Optics communications* (1980).